Supporting Information

Lee et al. 10.1073/pnas.1201613109

SI Materials and Methods

Conjugation of FtsK Trimer to Quantum Dots. Streptavidin-quantum dots (QDs) were purchased from Invitrogen (705 nm emission, Q10161MP, Invitrogen). Biotinylated FtsK was diluted to 20 nM (in trimers) and incubated with 20-fold excess of streptavidin-QDs in binding buffer [40 mM Tris·HCl (pH 8.0), 100 mM NaCl, 2 mM MgCl$_2$, 0.2 mg mL^{-1} BSA, 2 mM DTT] for 10 min on ice. QD-conjugated FtsK-trimers were diluted in binding buffer supplemented with 0.3 nM YOYO-1 (Invitrogen), 1.4 mM glucose, glucose oxidase, catalase, and 1 mM nucleotides (where indicated) (1). FtsK was diluted to a working concentration of 10 pM in the presence of nucleotide or 100 pM in the absence of nucleotides. The higher concentration of FtsK required for reactions conducted in the absence of nucleotide cofactor reflects the reduced affinity of FtsK for DNA in the absence of nucleotide.

The QD labeling procedure involves the use of a 20-fold molar excess of QDs to FtsK trimer to tag the FtsK motors. This use of the large excess of QDs should minimize the possibility that multiple motors would bind to the same QD. Assuming that the binding of the FtsK trimers to the QDs follows a Poisson distribution, then at a 1:20 protein to QD ratio (20 nM FtsK trimer: 400 nM QD) the probability (P) that a QD has no protein bound is $P = 0.951$, the probability that a QD has one FtsK trimer bound is $P = 0.048$, the probability that a single QD has two trimers bound is $P = 0.001$, and the probability that a single QD has three or more trimers bound is $P = 0.00002$ (2); therefore most of the FtsK-QD complexes should have just one trimer of bound FtsK before loading on the DNA. Please note that this calculation assumes that FtsK does not oligomerize before being coupled to the QDs. If FtsK forms a hexamer in solution, then the probabilities scale accordingly (i.e., the probability of two hexamers per QD is $P = 0.0005$).

DNA Substrates for Single-Molecule Experiments. FtsK activity is guided by the 8-bp KOPS sequence (FtsK Orienting/Polarizing Sequence; 5′-GGGNAGGG-3′) (3). Our experiments used a recombinant bacteriophage λ-DNA substrate that contained KOPS (5′-GGGCAGGG-3′ at ≈10.2 kb, 5′-GGGAAGGG-3′ at ≈38.3 kb) and an overlapping triple KOPS repeat (3xKOPS; 5′-GGGCAGGGCAGGGCAGGG at ≈28.5kb) (4). The 3xKOPS is frequently used as a strong FtsK-binding sequence (4, 5). The total length of the recombinant DNA substrate was 48,571 bp (Fig. 1*B*).

All λ-phage DNA cloning was carried out in vivo using a Red system-based recombineering method (6). Phage DNA harboring the *cI857* and *S7* mutations (New England Biolabs) was packaged (MaxPlax extract; Epicentre Biotechnologies), and high-titer viral stocks were prepared by plate lysis (7). To generate lysogens, *Escherichia coli* strain 7723 was infected with λ-phage at a multiplicity of infection of >10. Lysogens were identified by two rounds of replating colonies at both permissive (32 °C) and nonpermissive (42 °C) temperatures.

DNA inserts were prepared by PCR amplification of a custom plasmid DNA sequence (Dataset S1) using oligos IF01 and IF02 (Table S1). The ≈4.5-kb DNA insert was carefully selected to lack all KOPS-like sequences and to encode the *bla* ampicillin resistance gene as a selectable marker. The 5′ end of IF01 contained a 50-bp homology to λ-DNA as well as the 3xKOPS sequence. The 5′ end of IF02 also harbored a 50-bp homology to a downstream region to λ-DNA. The DNA insert was targeted to replace a region of the phage genome that is completely dispensable for viability. The PCR product was cleaned up using a purification kit (QIAquick; Qiagen).

Recombineering was carried out essentially as previously described (6). Briefly, lysogens were transformed with pKD78, a plasmid that contains the arabinose-inducible Red recombination system (8). Lysogens were grown at 32 °C in the presence of 0.2% arabinose and 34 μg mL^{-1} chloramphenicol to an OD$_{600}$ ≈0.4, washed with ice-cold water at least three times, and electroporated with the desired PCR product. After electroporation, cells were immediately resuspended in 1 mL of room temperature super optimal broth with catabolite repression (SOC) medium and allowed to grow overnight with shaking at 32 °C. Cells were plated on carbenicillin plates (30 μg mL^{-1}) and grown at 32 °C overnight. Colony PCR and DNA sequencing confirmed the presence of the desired insert and 3xKOPS sequence. Phage particles were isolated from heat-inducible *E. coli* lysogens, and λ-DNA was purified according to standard protocols (9).

For the experiments presented in Fig. S7, 3xKOPS-containing λ-DNA was amplified by PCR using oligos JL01 and JL02. The PCR products were inserted via recombination as described above. In this construct, 110 bp including 3xKOPS was deleted from the 3xKOPS λ-DNA (total 48,461 bp).

Phage DNA with one biotionylated *cos* end and one digoxigenin-containing *cos* end was prepared according to previously published protocols (10). Briefly, the *cos* ends were annealed with oligos IF03 and IF04 (Table S1), ligated, and filtered over a Sephacryl S-1000 column (GE Healthcare) to remove excess oligonucleotide and ligation reaction components.

FtsK Binding Distribution Histograms. Double-tethered DNA curtains were prepared as previously described (11), with the exception that we used "zig-zag"-shaped barriers to align the DNA molecules (12) rather than linear barriers (Fig. S1). QD-labeled FtsK was injected into the flowcell and allowed to equilibrate with the DNA for >30 s. Images were then collected for 200 s at a frame rate of 10 frames per second using NIS-Elements software (Nikon) and stored as uncompressed TIFF files. After data collection, the positions of barriers and pentagons were verified by white-light illumination. DNA-bound FtsK molecules were then identified manually, and only individual molecules were selected on the basis of the blinking of the QD signals; any QDs that did not exhibit blinking were excluded from the analysis. QDs that were visible for <5 s were also excluded from the binding histogram analysis, therefore the binding distributions only reflect the population of proteins that stably associated with the DNA. For all binding distribution histograms built from experiments performed in the absence of ATP, the binding position of each FtsK molecule was computed by averaging 200 consecutive video frames, which reduced localization uncertainty due to DNA fluctuations, and the locations of the QD-tagged proteins were determined by fitting the resulting images with a 2D Gaussian function to determine subpixel localization, as previously described (13). The positions of FtsK along the DNA were then mapped by measuring the distance from the center of the nanofabricated barrier to the localized QD signal. The conversion factor from pixels to base pairs was computed by dividing the distance between the center of top and bottom barriers and the DNA length. All histograms were constructed using Origin 8.0 with a bin size of 1.2 kb. Error bars were calculated by bootstrapping the data and indicate a 70% confidence interval (14).

FtsK Binding Distribution Histograms in Reactions with ATP. FtsK moves along DNA when it is capable of hydrolyzing ATP.
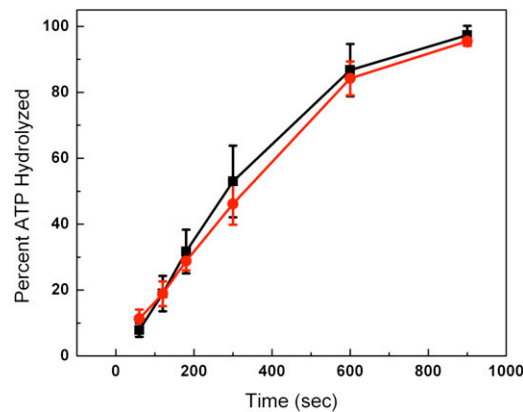
Therefore, we only included data reflecting the initial binding positions of FtsK before extensive translocation. First, FtsK was injected into a sample chamber with buffer containing ATP (as indicated) while movies were being recorded. Second, kymograms built from the resulting videos were used to identify proteins that underwent active ATP-mediated translocation (representing ≈90% of the total population). Third, from these kymograms we identified the first video frame in which the proteins could be detected on the DNA; this first frame represents the experimentally detected initial binding of FtsK to the DNA. Fourth, once the frame containing the initial binding event was identified, the QD signal from this frame was fit to a 2D Gaussian to locate the position of the protein on the DNA. As with the binding distributions built from data collected under conditions whereby FtsK does not translocate (described above), the positions of the protein along DNA were computed by measuring the distance from the center of the top nanofabricated barrier to the localized QD signal. The conversion factor from pixels to base pairs was computed by dividing the distance between the center of top and bottom barriers and the DNA length. All histograms were constructed using Origin 8.0 software using a bin size of 1.2 kb. Error bars were estimated by bootstrapping the data and indicate a 70% confidence interval. Note that because ATP is present in these experiments, FtsK may be translocating while the EM CCD is integrating this first image. However, any potential movement of FtsK during this first 100 ms is insufficient to explain the drastically different binding distributions observed in the presence of ATP (Fig. 3). Rather, if FtsK were binding to KOPS and then translocating away from KOPS during acquisition of a single video frame, then we would simply expect the KOPS binding peaks to shift at most by 500 bp ($\approx$5-kb s^{-1} translocation × 0.1-s image acquisition) to the left or right (as dictated by the orientation of KOPS).

Tracking vs. Position Mapping Precision. Tracking precision describes how accurately we can track the relative frame-to-frame variation in the position of an individual QD-tagged protein, which is primarily a function of the signal to noise ratio, as determined by the brightness of the QDs, as well as the photon collection and detection efficiency. In the experiments reported here, tracking precision was typically ±30 nm. Position mapping precision describes how accurately we are able to map the binding position of the protein population relative to the underlying DNA sequence. In the experiments reported here our mapping precision is reflected in the widths of the KOPS binding site peaks in the distribution histograms. The factors that contribute to the peak width include (i) the tension on the DNA (in all of our double-tethered DNA experiments the DNA is only extended to a mean length of ≈70–80%; we do this intentionally so as to avoid overstretching the DNA), (ii) the alignment of the DNA molecules relative to one another at the leading edges of the zig-zag–shaped barriers, (iii) the amount of protein binding to non-KOPS sites relative to KOPS sites for a particular experimental condition, and (iv) the number of molecules used to generate the distribution histograms.

1. Ha T, et al. (2002) Initiation and re-initiation of DNA unwinding by the *Escherichia coli* Rep helicase. *Nature* 419:638–641.
2. Block SM, Goldstein LS, Schnapp BJ (1990) Bead movement by single kinesin molecules studied with optical tweezers. *Nature* 348:348–352.
3. Sherratt DJ, Arciszewska LK, Crozat E, Graham JE, Grainge I (2010) The *Escherichia coli* DNA translocase FtsK. *Biochem Soc Trans* 38:395–398.
4. Sivanathan V, et al. (2006) The FtsK gamma domain directs oriented DNA translocation by interacting with KOPS. *Nat Struct Mol Biol* 13:965–972.
5. Graham JE, Sherratt DJ, Szczelkun MD (2010) Sequence-specific assembly of FtsK hexamers establishes directional translocation on DNA. *Proc Natl Acad Sci USA* 107:20263–20268.
6. Sharan SK, Thomason LC, Kuznetsov SG, Court DL (2009) Recombineering: A homologous recombination-based method of genetic engineering. *Nat Protoc* 4:206–223.
7. Lech K (2001) Growing lambda-derived vectors. *Curr Protoc Mol Biol*, Chapter 1:Unit 1.12.
8. Datsenko KA, Wanner BL (2000) One-step inactivation of chromosomal genes in *Escherichia coli* K-12 using PCR products. *Proc Natl Acad Sci USA* 97:6640–6645.
9. Lech K, Reddy KJ, Sherman LA (2001) Preparing lambda DNA from phage lysates. *Curr Protoc Mol Biol*, Chapter 1:Unit 1.13.
10. Finkelstein IJ, Greene EC (2011) Supported lipid bilayers and DNA curtains for high-throughput single-molecule studies. *Methods Mol Biol* 745:447–461.
11. Gorman J, Fazio T, Wang F, Wind S, Greene EC (2010) Nanofabricated racks of aligned and anchored DNA substrates for single-molecule imaging. *Langmuir* 26:1372–1379.
12. Visnapuu ML, Fazio T, Wind S, Greene EC (2008) Parallel arrays of geometric nanowells for assembling curtains of DNA with controlled lateral dispersion. *Langmuir* 24:11293–11299.
13. Gorman J, et al. (2007) Dynamic basis for one-dimensional DNA scanning by the mismatch repair complex Msh2-Msh6. *Mol Cell* 28:359–370.
14. Efron B, Tibshirani R (1993) *An Introduction to the Bootstrap* (Champman and Hall, New York).

Fig. S1. Double-tethered DNA curtains with defined lateral dispersion. (*A*) *Left*: Optical image of the nanofabricated structures for a double-tethered DNA curtain with a zig-zag–shaped geometric barrier for aligning DNA molecules within single "nanowells" and downstream pentagonal anchor points for tethering the second end of the DNA. *Right*: A more detailed view of the pattern elements; white arrows illustrate how the apex of each "nanowell" is aligned with one pentagonal anchor. The distance between the adjacent "nanowells" is 1.5 μm. (*B*) Histogram of observed distances between adjacent YOYO1-stained DNA molecules within the double-tethered curtains. The histogram was fit with five Gaussian functions, and as illustrated here the peak-to-peak distances between adjacent DNA molecules with the curtains occurred at multiples of ≈1.5 μm, as expected for this DNA curtain design (1, 2). The DNA separation distances presented here are reflective of the typical DNA curtains used in the FtsK experiments.

1. Visnapuu ML, Fazio T, Wind S, Greene EC (2008) Parallel arrays of geometric nanowells for assembling curtains of DNA with controlled lateral dispersion. *Langmuir* 24:11293–11299.
2. Greene EC, Wind S, Fazio T, Gorman J, Visnapuu ML (2010) DNA curtains for high-throughput single-molecule optical imaging. *Methods Enzymol* 472:293–315.

Fig. S2. Assessment of in vivo biotinylation of FtsK. FtsK (0.2 pmol) was mixed with increasing amounts of streptavidin (SA) and incubated in standard microscope buffer [40 mM Tris (pH 8), 0.2 mg/mL BSA, 1 mM DTT, 50 mM NaCl] for 20 min on ice. SDS/PAGE loading buffer was then added to the samples, but the samples were not boiled to maintain the biotin-streptavidin interaction. Reactions were resolved on an 8% SDS/PAGE gel at 250 V for 80 min, and protein bands were detected with SimplyBlue SafeStain (Invitrogen). Lanes: 1, molecular mass standards; 2, FtsK only; 3, 1:1 FtsK:SA; 4, 1:3 Ftsk:SA; 5, 1:10 FtsK:SA; 6, 1:30 Ftsk:SA; 7, 1:100 FtsK:SA; 8, 1:300 Ftsk:SA. These gel shift assays revealed that >90% of the trimers were biotinylated.

Fig. S3. ATPase activity of QD-tagged FtsK. ATP hydrolysis reactions were conducted at room temperature in buffer containing 40 mM Tris (pH 8), 0.2 mg/mL BSA, 1 mM DTT, 50 mM NaCl, 2 mM $MgCl_2$, 1 nM lambda phage DNA, 1 mM ATP, and 100 pM FtsK trimer. Reactions were terminated at the indicated time points by the addition of an equal volume of 50 mM EDTA. The products were then resolved by TLC and quantified with phosphor imaging. The black curve represents reactions in the absence of QDs, and the red curve represents reactions conducted at a 1:20 ratio of FtsK:streptavidin-QDs. Error bars denote the SD of at least three independent measurements.
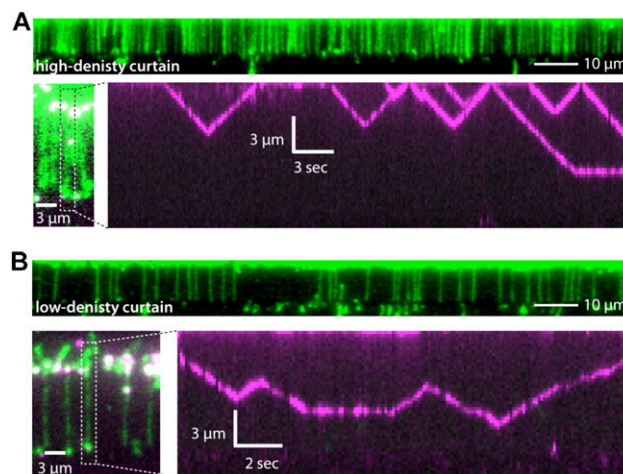

Fig. S4. FtsK reverses directions irrespective of DNA curtain density. FtsK translocation experiments were performed on DNA curtains with differing amounts of DNA. (*A* and *B*) *Upper*: Examples of high- and low-density DNA curtains, respectively. *Lower*: Examples of specific individual DNA molecules; the corresponding kymograms show the behavior of FtsK on these different DNA molecules. In *A* the distance between the nanowells was 1.5 μm, although the DNA was loaded at such a high density that there may be more than one DNA molecule present per nanowell. In *B* the DNA was loaded at a low density, and for the highlighted molecule the nearest neighboring DNA molecules were 3 μm to the left and 6 μm to the right. As shown in the kymograms, FtsK reversed direction during translocation irrespective of the DNA curtain density. The low-density DNA curtain in *B* is typical of that which was used for all of the experiments presented in the main text. These findings indicate that the changes in direction were independent of local DNA curtain density, indicating that FtsK remained bound to the same DNA molecule for the duration of the experimental observations, and arguing against the possibility that the changes in direction resulted from FtsK "jumping" to a nearby DNA molecule.

Fig. S5. FtsK changes direction in the absence of free proteins. First, 1 pM of QD-tagged FtsK was bound to a DNA curtain in buffer containing 1 mM ADP. The sample chamber was then flushed with buffer lacking free FtsK for ≈3 min at a flow rate of 0.3 mL/min. This washing procedure removed all detectable traces of free QD-tagged FtsK, as judged by the absence of free quantum dots diffusing within the sample chamber. After identifying molecules of KOPS-bound FtsK, translocation was then initiated by flushing the sample chamber with buffer containing 1 mM ATP. As illustrated by the kymogram, FtsK still exhibited changes in direction during translocation, even after flushing the chamber to remove free proteins, arguing against the possibility that the changes in direction arose from collisions with other, transiently bound molecules of FtsK.
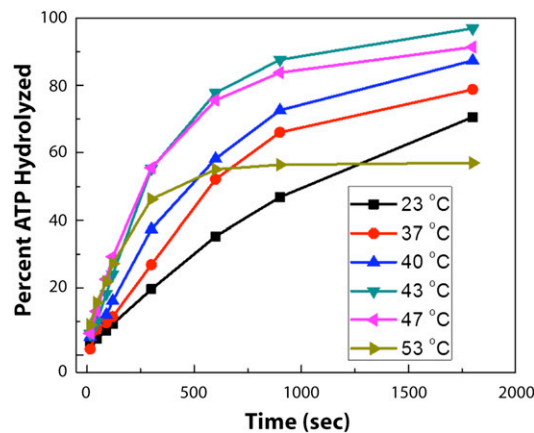
Fig. S6. Temperature dependence of the FtsK ATPase activity. ATP hydrolysis reactions were conducted as described in Fig. S2 at temperatures ranging from 23 °C to 53 °C, as indicated.
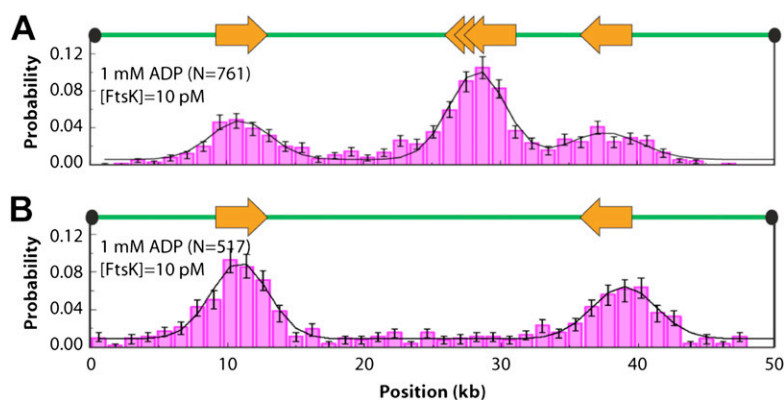
Fig. S7. KOPS specificity of FtsK DNA binding activity. (*A*) Binding distribution of FtsK on the 3xKOPS bearing λ-DNA substrate; note that this panel is identical to that shown in Fig. 3*A* from the main text. (*B*) Binding distribution of FtsK on a λ-DNA substrate lacking the 3xKOPS site. As shown here, when the 3xKOPS site is not present, the middle peak in the FtsK binding distribution disappears, confirming that the peak can be ascribed to KOPS-specific binding by FtsK.
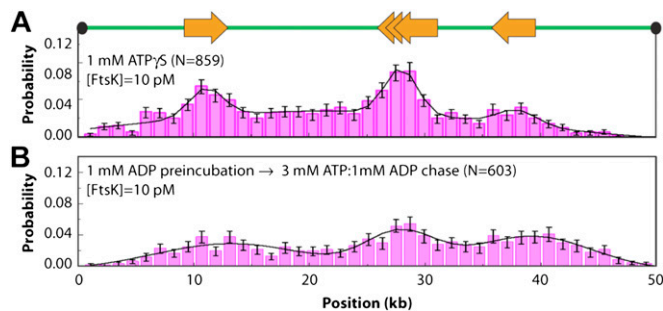
Fig. S8. Binding distribution histograms of FtsK under different nucleotide conditions. (*A*) Wild-type FtsK binding distribution with 1 mM ATPγS. (*B*) Wild-type FtsK binding distribution following a 20-min preincubation with 1 mM ADP followed by a chase with 3 mM ATP immediately before injection into the sample chamber.

Fig. S9. Overview of procedure for measuring initial binding distribution histograms for the translocating FtsK molecules. (*A*) Typical kymogram of a translocating molecule of FtsK collected in the presence of 1 mM ATP. The circled region indicates the first frame in which the protein is detected bound to the DNA. (*B*) Video frame corresponding to the initial Ftsk binding event, along with an example of (*C*) 2D Gaussian fit, which is used to pinpoint the location of the QD-tagged protein. (*D*) FtsK distributions measured in the presence of ATP (this panel is taken from Fig. 3*D*); the bin assignment for the protein shown in *A* and *B* is highlighted with an arrow. As indicated in the main text, KOPS binding dictates the direction of translocation, therefore if translocation influenced the outcome of these measurements, we would have expected the binding distribution peaks to shift ≈0.5 kb in the direction dictated by KOPS rather than disappear altogether.

Table S1.   Oligonucleotides

Name	Sequence
IF01	AAACGAATGCTGCAGCGTCACAACAATCAGCCGCCACGTCTGCCTCC accggtGGGCAGGGCAGGGCAGGGCACGTCTACAAGAAAGC
IF02	CAAACACAGAGCTCTTCATCATTTCAAGCTATTAAATATTGCTAACAG GTGCGCATAATGTATATTATGTTAAATCTGCTCTGATGCCGC
IF03	[P]AGGTCGCCGCCC[B]
IF04	[P]GGGCGGCGACCT[D]
JL01	TTTCTCTGTGCCATGACGGAGGATGATGCCCGGCCGGAGGTGCTGCGT CGTAAGGGTCTACTCGGTGGC
JL02	AGGACACACCCTCTTGAGC

Phosphates at 5′ positions are marked with a [P]. Biotin at the 3′ end is marked with a [B]. Digoxigenin at the 3′ end is marked with a [D]. The 3xKOPS sequence is underlined.

Other Supporting Information Files

Dataset S1 (TXT)